



Virginia Commonwealth University
VCU Scholars Compass

Theses and Dissertations


Graduate School

2018

Directing Mesenchymal Stem Cells for Periodontal Regeneration

Charles Stoianovici
Virginia Commonwealth University

Follow this and additional works at: <https://scholarscompass.vcu.edu/etd>

 Part of the [Periodontics and Periodontology Commons](#)

© The Author

Downloaded from

<https://scholarscompass.vcu.edu/etd/5335>

This Thesis is brought to you for free and open access by the Graduate School at VCU Scholars Compass. It has been accepted for inclusion in Theses and Dissertations by an authorized administrator of VCU Scholars Compass. For more information, please contact libcompass@vcu.edu.

© Charles Stoianovici _____ 2018
All Rights Reserved

Directing Mesenchymal Stem Cells for Periodontal Regeneration

A thesis submitted in partial fulfillment of the requirements for the degree of Master of Science
in Dentistry at Virginia Commonwealth University

By

Charles Stoianovici

University of California Irvine 2009

Western University of Health Sciences School of Dentistry 2015

Director: Zhao Lin

Assistant Professor, Department of Periodontics

Virginia Commonwealth University

Richmond, Virginia

May 2018

Acknowledgement

I would like to thank my committee members, Dr. Zhao Lin, Dr. Al Best, Dr. Harvey Schenkein, and Dr. Thomas Waldrop for their mentorship and guidance in the development of this research.

I would also like to thank Dr. Chongxia Yue, Dr. Jie Cao, Dr. Mingxu Sun, Dr. Josh Cohen, Sonia Talegaonkar, and Maya Harrington for their support and help with the research project. I wish to express my deepest appreciation to my wife Christina and my parents Toma and Eva, who have supported and encouraged me throughout this journey.

Table of Contents

Abstract	vii
Introduction.....	1
Periodontal Disease.....	1
Guided Tissue Regeneration and Periodontal Regeneration	3
Bone Substitutes.....	5
Biologics	7
Emerging Concepts.....	8
Specific Aims.....	12
Methods and Materials.....	13
Aim 1: E7- Peptide In-vivo Release Kinetics	13
Aim 2: Osteoinductive potential of DBM in Combination with E7	15
Statistical analyses	18
Results.....	19
Aim 1: Retention of E-7 Peptide on HA discs	19
Aim 2: The osteogenic potential of bone graft material combined with E7HA peptide	19
Discussion.....	22
Conclusion	29
Appendices.....	30

Appendix 1: Conflict of interest Disclosure 30

Bibliography 31

Tables 37

Figures..... 39

List of Tables

Table 1. Fluorescence Intensity by Peptide Coating Group at Each Week	37
Table 2. New Bone Volume, by Groups.....	37
Table 3. Paired Comparisons between Groups	38

List of Figures

Figure 1: Disc mplantation in Animals and Fluorescent Imaging in Aim 1	39
Figure 2: In-vivo Fluorescence Readings at 0,2,4, and 8 Weeks.....	40
Figure 3: Sky Scan 1173 Micro-CT and Gastrocnemius Implantation Protocol	40
Figure 4: Active DBM MicroCT Ectopic Bone Formation	41
Figure 5: Inactive DBM MicroCT Ectopic Bone Formation.....	41
Figure 6: Active DBM E7-Heptaglutamate MicroCT Ectopic Bone Formation.....	43
Figure 7: Inactive DBM E7-Heptaglutamate MicroCT Ectopic Bone Formation.....	44
Figure 8: Fluorescent Intensity by Peptide Coating Group at Each Week	45
Figure 9: Fluorescence Intensity by Peptide Coating Group at Each Week.....	46
Figure 10: New Bone Volume (mm ³).....	47
Figure 11: Inactive DBM Histology Sample	48
Figure 12: Active DBM Histology Sample	48
Figure 13: Inactive DBM-E7 Histology Sample	49
Figure 14: Active DBM-E7 Histology Sample.....	50
Figure 15: Active DBM-E7 Histology New Bone Formation	50

Abstract

DIRECTING MESENCHYMAL STEM CELLS FOR PERIODONTAL REGENERATION

By

Charles Stoianovici

A thesis submitted in partial fulfillment of the requirements for the degree of Master of Science in Dentistry at Virginia Commonwealth University.

Virginia Commonwealth University, 2018

Major Director: Zhao Lin

Assistant Professor, Department of Periodontics,

Virginia Commonwealth University School of Dentistry

Background: Directing autogenous Mesenchymal Stem Cell (MSC) to defect sites has a great promise in bone regeneration. We designed a MSC specific, bone affinity peptide (E7HA7) by conjugating E7 with a polyglutamate hydroxyapatite (HA) binding motif. We sought to characterize the in-vivo releasing pattern and bioactivity of E7HA7. **Methods:** HA discs were coated with fluorescent labeled peptides E7HA7, E7HA2 or E7 were subcutaneously implanted

in Sprague Dawley rats. In an ectopic bone formation model was used to test the in-vivo bioactivity of E7HA7 conjugated to DBM. **Results:** E7HA7 showed slower peptide release from scaffolds in comparison to other groups, being statistically significant at week 2 compared to E7, and to E7HA2 at week 4 and 8. In ectopic model, the medians for new bone formation in each group were: iDBM=0.041mm³, iDBM-E7=0.071mm³, aDBM=0.138mm³, and aDBM-E7=0.192mm³. **Conclusions:** Conjugation of E7 to polyglutamate bone binding domain showed slow releasing kinetics and osteoinductive potential.

Keywords: Mesenchymal Stem Cell, Regeneration, Hydroxyapatite, Demineralized Bone Matrix, Peptide

Introduction

Periodontal Disease

Periodontal disease is one of the most common inflammatory diseases affecting over 50% of adults in the United States¹. It is characterized as inflammation of the supporting tissues of teeth, which can progressively lead to periodontal pocket formation, suppuration, fibrosis, destruction of alveolar bone and periodontal ligament (PDL), mobility and eventual tooth exfoliation. In a study by Becker et al, when periodontal disease remained untreated, patients continued to have progressive radiographic bone loss and increased in probing depth. When periodontally hopeless teeth were not treated, patients were at risk of losing 0.36/teeth per year². However periodontal disease can be managed with numerous therapies including non-surgical therapy, surgical therapy, and regenerative methods.

The primary etiological factor in periodontitis is bacterial biofilm and their products, which cause inflammatory reaction by the host. Eventually, with the continued host mediated destruction, patients begin to have an apical migration of the junctional epithelium leading to pocket formation and possible bone loss. With bone loss and apical migration of the junctional epithelium, pocket formation will continue to propagate forming a favorable anaerobic environment for bacterial biofilm. In addition to the favorable environment for anaerobic bacterial species, the bone loss often creates osseous defects in between teeth that makes treatment even more challenging for the clinician.

The goal of periodontal treatment is to arrest the progression of periodontal disease and if possible reverse some of the effects with regenerative therapies. Removal of the harmful bacterial biofilm is completed through scaling and root planing. Scaling and root planing utilizes periodontal scalers and curettes to mechanically remove plaque and calculus off tooth and root surfaces, and then smooth out root surfaces to remove infected dentin and cementum that can be

impregnated with etiological factors that cause inflammation. Scaling and root planing is the primary and initial modality of treating periodontitis, however, the effectiveness of the non-surgical treatment can be limited by the severity of periodontal disease and numerous local factors such as cervical enamel projection (CEP), root grooves, enamel pearls, cemental tears, furcations, etc. The efficacy of scaling and root planing is dependent on the initial probing depths. In deep, > 6 mm pockets, only 32% of the surface were calculus free after Scaling and root planing group. On average, scaling and root planning was shown to reduce probing depths by 1.56 mm and have an attachment gain of 0.52 mm³. However, even with the reduction in probing depth and gains in attachment, long term studies have shown that over time non-surgical therapy is not as effective as surgical therapy especially as the severity of periodontal disease increases ^{4,5}.

Non-surgical therapy is the initial step for managing periodontal diseases, which usually results in a repair of the periodontium with the attachment of long junctional epithelium to root surface. The curetted root surface may be repopulated by 4 different types of cells: epithelial, gingival connective tissue, bone and PDL cells. Depending on the cells which repopulate the root surface, different attachments may form. Long junctional epithelium healing has no new CT attachment and is just epithelial downgrowth (reattachment). However, if new CT attachment is formed through repopulation by PDL, then new attachment can occur. Similar healing occurs through surgical therapy however there is increased probing depth reduction at the expense of attachment levels. In more severe cases of periodontitis intrabony defects, depending on the morphology of defects it can be treated with regeneration. The term regeneration is defined as the reconstitution of a lost or injured part, which in periodontics would be the reconstitution of the periodontal ligament, cementum and bone.

Guided Tissue Regeneration and Periodontal Regeneration

Guided tissue regeneration attempts to regenerate the lost periodontal structure by excluding the epithelium from the root surface allowing for bone, cementum, and PDL to regenerate. The idea that the PDL has the ability to regenerate was originally proposed by Melcher where he hypothesized that the periodontium has four separate compartments of connective tissue (CT) in the periodontium: the gingival corium, periodontal ligament (PDL), cementum, and bone^{6,7}. Therefore, for regeneration to occur, the regeneration of periodontium must come from the bone and PDL. The PDL tissue contains a population of Mesenchymal Stem Cells (MSCs) which are multipotent stromal cells that can differentiate into multiple cell lineages. Mesenchymal stem cells are essential for osteogenesis and cementogenesis in the development of the periodontium which give rise to cementoblasts, osteoblasts, fibroblasts, myofibroblasts, endothelial cells nerve cells and epithelial cells. The multipotentiality of MSCs is believed to be crucial for regeneration⁸.

The regenerative potential of the periodontal ligament was demonstrated by Nyman in monkeys with guided tissue regeneration technique, which showed that by excluding the epithelium in surgically created defects, the preference was given to periodontal cells to repopulate the area and regenerate the periodontium⁹. The limitation of the study was that the site was not previously diseased and that the defects were created surgically. Gottlow, later demonstrated that with previously diseased root surfaces it was also possible to regenerate the periodontium¹⁰. With epithelial exclusion, coagulum is formed and inflammatory cells infiltrate the area removing necrotic tissue¹¹. MSCs from nearby bone marrow and periodontal ligament then migrate into the defects and begin to differentiate into tissue specific cells such as osteoblasts, PDL cells and cementoblasts. At the same time, tissue specific extracellular matrix is

produced. With the formation of blood vessels more MSC's are brought to the defect, with eventual regeneration of the periodontal complex. The origin of the regenerative cells was confirmed by Iglhaut through histologic and autoradiographic analysis, indicating that bone and PDL tissue compartments supply cells to a periodontal wound in surgically created periodontal spaces¹². The mesenchymal stem cells embedded within the bone and PDL are the at the center of the regenerative events, and often these cells are considered as a reservoir for healing-promoting factors because of their trophic and immune-modulatory activities¹³. The need for MSCs is vital for regeneration otherwise the defect will be dominated by fibrotic cells leading to non-functional scar tissue, referred to as tissue repair.

Over the years numerous techniques have been developed to regenerate periodontal tissues, including placing graft substitute material within a periodontal defect in combination with some type of resorbable or non-resorbable periodontal membrane, membrane alone, bone substitute in combination with biological material, biological material alone, etc. Although successful results were observed, they are highly unpredictable and the outcome is still largely depend on defect morphology(depth, width, number of walls), particulate size, ability of surgeon, correct material chosen for the defect, stability of graft, ability for angiogenesis, sufficient space for progenitor cells to populate the area, and stability of the periodontal complex¹⁴. In Froum's study where osseous coagulum was compared versus open flap debridement it was showed that bone fill was an average 3.64mm in 3 wall defects, 3.21mm in 2 wall defects, and 2.42mm in 1 wall defects, whereas open flap debridement showed 1.38mm, 1.03mm, and 0.16mm respectively¹⁵. Although the grafted sites were deeper in this study, it does show that the more bony walls a defect has the better regenerative potential is possible due to greater surface area and access to MSCs from the bone and periodontal ligament. Similarly, using Gore-tex

membrane Cortellini showed that 3 wall defects were filled by $95\pm 6.2\%$, 2 wall defects were filled by $82\pm 18.7\%$ and 1 wall defects was only filled by $39\pm 62.4\%$. These results again show that the increased number of bony walls the better regenerative outcome is possible¹⁶. Lastly, in furcations, Murphy and Gunsolley demonstrated in their systematic reviews and meta-analysis that class 2 furcations have the best regenerative outcomes, due to the ability to have sufficient space to maintain and stabilize graft material within the sites¹⁷. It was found that within class 2 furcations both membrane and graft material enhanced vertical probing depth reduction, horizontal attachment level, and horizontal open attachment level gain¹⁷. Often clinicians are faced with varying morphological defects that are not ideal. Such irregular defects present a significant challenge for regeneration, partly might due to a decreased access to mesenchymal cells from the neighboring bone and periodontal ligament.

Bone Substitutes

Bone substitute materials vary from autografts (cortical/cancellous bone, bone marrow), allografts (demineralized freeze-dried/freeze-dried bone), xenograft, and alloplastic materials (ceramics, hydroxyapatite, polymers and bioglass). New bone formation can occur by three mechanisms utilizing bone substitute materials can occur by three mechanisms: osteogenesis osteoinduction, osteoconduction. Osteogenic potential is defined as the ability to have vital osteoblasts within the grafting material that allow for bone formation. Osteoinduction is defined as the stimulation of osteoprogenitor cells (mesenchymal cells) to differentiate into osteoblasts that produce new bone formation. Osteoconduction refers to the grafting material acting as a scaffold for new bone formation from host bone cells. Autografts have osteogenic, osteoconductive and osteoinductive potential. Allografts have osteoconductive and osteoinductive potential depending on the amount of mineralization within the graft, and lastly

alloplastic materials are limited to an osteoconductive potential. In periodontal regeneration, autogenous bone and bone marrow is the “gold standard” of grafting because there are MSCs within the graft which can differentiate into multiple cell types favoring the regeneration process. However, the limitation to autogenous grafting is that often a second site is needed, increased patient morbidity, insufficient autogenous bone, and poor quality autogenous bone.

As a substitute to autogenous bone, allografts are a common substitute used to fill osseous defects and can come in a combination of mineralized freeze-dried bone allograft (FDBA) and demineralized freeze-dried bone allograft (DFDBA). In early regeneration studies DFDBA was used for periodontal defects because of its osteoinductive ability. Urist and Strates first demonstrated that demineralized bone has osteoinductive potential through bone formation in extraskeletal sites¹⁸, which led clinicians to believe that DFDBA is an excellent material bone substitute. The osteoinductive potential is from remaining bone morphogenic proteins in the processed graft, where it was shown that BMP-2, BMP-4, and BMP-7 are present¹⁹. Osteoinductive capabilities of DFDBA often vary between tissue banks and same batches of graft material, which could be due to inactive proteins within the graft, insufficient quantities, processing methods, age of donor, and medical status^{20,21,22}. Initially it was believed that due to presence of BMP within DFDBA, the bone graft would be superior in regeneration, which was shown in early studies²³, however based on meta-analysis and various clinical studies there was no difference in the ability to treat intrabony and furcal defects²⁴⁻²⁶. The lack in superiority of DFDBA over FDBA is due to the heterogeneous nature of the studies, processing methods used by different tissue banks, variance in surgical skill, etc

A substitute to allografts and autografts are alloplasts, which are synthetic inert bone substitutes. A commonly used alloplast is hydroxyapatite which is made of calcium phosphate,

the primary constituent of bone mineral. Alloplasts have been used for regeneration based on properties of being highly adsorptive and osteoconductive. Although numerous bone substitute grafts can be used for periodontal regeneration, they are often osteoconductive and not inductive and do not have the potential to induce neighboring MSCs for regeneration, therefore supplemental biological materials can be added to the graft to improve the osteoinductivity.

Biologics

Although bone substitute materials are commonly used in periodontal defects, there is still clinical unpredictability, therefore additional materials such as biologics can be added to bone substitutes or be used alone for regeneration. The biologics can range from the delivery of stem cells or different recombinant proteins consisting of Enamel Matrix Derivative (EMD), platelet rich plasma (PRP), bone morphogenic proteins (BMP), platelet derived growth factor (PDGF), or synthetic peptides²⁷ One of the most commonly used biologics is EMD, which is a protein/peptide mix derived from porcine teeth. EMD induces cementogenesis and is a tissue healing modulator that helps stimulate periodontal regeneration. EMD has been shown to be effective in periodontal regeneration alone or in combination with bone graft substitutes. Platelet derived growth factor (PDGF) is derived from platelets, macrophages, and osteoblasts. PDGF stimulates intracellular pathways for DNA and protein synthesis and stimulate cell proliferation. It has been used in both periodontal and periimplant defects. Although both EMD and PDGF have been shown to be effective in periodontal regeneration and healing, limitations remain regarding the application of growth factors. EMD has a gel like consistency and if primary closure of the defects is not obtained the displacement of the growth factors takes place and often the gel like consistency is not sufficient in maintaining space within the defect leading to soft

tissue collapse. Additionally, the varied results in literature may be due to a low efficiency in targeting MSCs to allow further expansion and functioning during the healing process.

Even with modern biologics, the degree of tooth-supporting tissue regeneration is still suboptimal and usually results in less than 50% bone regeneration and 20% horizontal defect fill²⁸. One of the factors that makes regeneration unpredictable is the varying morphology that is encountered with each periodontal defect, inefficiency of directing MSCs into periodontal wound healing sites, and engraftment of MSCs which have made regeneration difficult²⁹. Periodontal regeneration is not a passive process, but rather a dynamic process that includes processes such as early protein expression, cell apposition, remodeling and maturation of the healing site⁸. Cell based therapies and homing of mesenchymal cells to accelerate and capitalize on the dynamic process of regeneration have drawn increasing attentions in the field.

Emerging Concepts

Cell therapy is being intensively investigated for accelerating periodontal regeneration through direct delivery of stem cells, mainly MSCs, to the periodontal defects. MSCs from bone marrow (BMSCs) are the most widely studied partly because they are easily accessible. Transplantation of BMSCs induced periodontal regeneration that was characterized by new cementum, bone and PDL ligament formation in experimental periodontal defects in rats, rabbits, mini pigs, and dogs³⁰. By cell-labeling techniques, the differentiation of exogenous BMSCs to cementoblasts, PDL fibroblasts, and alveolar bone osteoblasts was confirmed^{31,32}. Although a few preclinical and clinical studies have suggested the potential of MSC cell therapy in periodontal regeneration, many challenges remain in current treatment strategies based on exogenous stem cells. For example, a sophisticated cell culture facility is commonly needed for cell expansion before clinical use. There will be difficulties in the transportation of cells if a

central culture facility is used. Other issues include the lack of cell sources, safety concerns regarding the use of animal serum and potential tumorigenic effects. Furthermore, only a small percentage of stem cells remain after weeks of engraftment^{29,33}. Therefore, approaches to target endogenous MSCs in patients are highly desirable both from a clinical and financial standpoint.

Recently a MSC affinity peptide (E7, EPLQLKM) was discovered through phage display technology³⁴. The peptide showed a high affinity to BMSCs across rat and human species. E7 peptide has the ability to increase the homing and proliferation of MSCs^{36,37}, enhance the infiltration rate of stem cells³⁴, reduce inflammatory response³⁵, and promote ligament-bone healing and cartilage regeneration³⁵. Covalent conjugation of E7 to polycaprolactone (PCL) and poly-L-lactide (PLLA) bio-polymers significantly enhanced the attachment of BMSCs to the material surface and increased cell spreading. The E7 functionalized biomaterial was also able to stimulate MSCs proliferation during *in vitro* culture.³⁵ When bone marrow was cultured in the E7-conjugated cell culture devices, enrichment of MSCs was observed compared with those grown with E7, suggesting a use for MSC enrichment bio-incubators³⁶.

Recently, Lin group tested E7 peptide on human PDL cells against a scramble control (scramble sequence of E7) and DMSO to determine its affinity of PDL and BMSC cells. E7 was shown to have highest affinity for PDL progenitor cells and BMSC, and in addition E7 had a stronger affinity than RGD, a well investigated peptide of type 1 collagen. The affinity to PDL and BMSC was strong regardless of the modification of the terminal amino acid, suggesting a future protein engineering to modify the function of this peptide. Even though preliminary data shows strong affinity for PDL and BMSCs, from a clinical standpoint the addition of bone substitute material within periodontal defects allows space maintenance and tissue support for mesenchymal stem cells to migrate into the defect. Although it may seem logical to combine

peptides with bone grafts to induce greater bone growth, common issues with peptide therapy combined bone graft substitutes is the inability to have a controlled release of peptide. Often combination of growth factors with bone grafts results in a bolus release which can lead to immediate degradation and consumption of the peptide within a 24-hour period. In addition to the fact that growth factors have a very short half-life in vivo, superphysiological doses are commonly used in clinics. rhBMP-2 loading dose is usually a million times higher than physiological levels and many times higher than needed in non-human primates and mice.³⁷ Such high dosages of growth factors are often related to various systemic side effects as well as high treatment cost. Therefore, a peptide that has the ability to have a controlled release and strong bone conjugation would be able to promote a sustained regeneration.

As mentioned, hydroxyapatite is a widely used osteoconductive bone grafting material based on its similar structure to bone, and has been compatible with linking different peptides and proteins for bone regeneration^{38,39,40}. Numerous linking mechanisms to bone matrix have been identified from endogenous bone matrix proteins. For example, Osteocalcin⁴¹, Bone sialoprotein BSP⁴² and Osteonectin⁴³ bind to bone through γ -carboxyglutamic acid⁴¹. Such mechanisms inspired researchers to develop bone binding peptides/proteins. Phosphorylated amino acids or negatively charged amino acid sequences such as a poly-Asp chain⁴⁴ have been utilized to modulate bioactive peptides for stronger retention to hydroxyapatite. One binding mechanism utilizing polyglutamic acid allows different peptides to conjugate to bone/bone graft materials and increase the binding strength by nearly ten times⁴⁵, and allows for the retention of amino acids for up to 3 months in different allograft materials³⁶. Studies have not only shown that by increasing the number of glutamate residues³⁶ there is an increased binding strength to bone domains but by adjusting the number of glutamate residues, one can tune the release rate of

the amino acid. Utilizing the bone binding capabilities of polyglutamic acid and MSC homing ability of E7 peptide, we designed a novel peptide E7HA7 to improve the bioactivity of bone graft material by attracting and maintaining MSCs at the healing site. In this study, we investigated the in vivo bioactivity of this peptide.

Specific Aims

In this two-part study, we first tuned E7-HA with two glutamate residues (E7HA2) and seven glutamate(E7HA7) residues to determine which peptide modification has the greatest retention with hydroxyapatite in vivo. In part 2, we tested whether E7HA7 enhances the osteoinductive potential Demineralized Bone Matrix (DBM) in a murine ectopic bone formation model. Our hypothesis is that a greater retention of peptide E7 will occur with the heptaglutamate residue based on the greater number of anionic sites from glutamate. In aim 2 our hypothesis is that the conjugation of E7HA7 with DBM will enhance the osteoinductivity of the bone substitute material.

Methods and Materials

Aim 1: E7- Peptide In-vivo Release Kinetics

Experimental Design

All procedures performed on animals followed protocols approved by the institutional Animal Care and Use Committee (IACUC) at Virginia Commonwealth University. Synthetic hydroxyapatite (HA) discs were used as a model to mimic mineralized bone grafts. One E7 peptide without any glutamate modifications was attached to the E7 directly and two HA binding domains, one with seven glutamates (E7HA7) and the other with two glutamates (E7HA2), were linked to the bone grafts. All peptides were labeled with Fluorescein isothiocyanate (FITC) fluorescent marker at the N terminus for in-vivo fluorescence detection.

Peptide Synthesis

Peptide synthesis: The following custom peptides were synthesized from Genscript Co. (Piscataway, NJ):

Name	Sequence
HA Disc	None (control)
E7	EPLQLKMCK-(FITC)
E7HA-2	EEEPLQLKMCK-(FITC)
E7HA-7	EEEEEEEEPLQLKMCK-(FITC)

In order to facilitate the conjugation of FITC to the peptides, a cysteine is added to N terminus. All peptides were reconstituted in DMSO to achieve a concentration of 2 mg/mL, aliquoted and stored at -20°C . HA disks (5mm in diameter, 1.6mm in thickness) that designed for 96-well plate were obtained from 3D-Biotek (Hillsborough, NJ, USA). To track binding and release kinetics, variations of these peptides were synthesized to contain Fluorescein (FITC) tags.

Peptide coating

The peptide solutions were added to HA scaffold in sterile 96 well plate (100 ul/well) with concentrations of 0.2 mM with continuous agitation at room temperature. After 24 hours, supernatants were aspirated completely and surfaces were briefly washed three times with phosphate buffered saline (PBS) for 5 min with agitation. The HA discs were dried and stored under sterile conditions at room temperature in a dark environment until needed.

Surgery

All procedures performed on animals followed protocols approved by the Institutional Animal Care and Use Committee (IACUC approved protocol number: AD10001162) at Virginia Commonwealth University. Animals were ordered two weeks ahead of time to allow rats to acclimate to the environment and were fed *ad libitum*. Rats were randomized by independent examiner and were weighed prior to anesthesia, at week 2,4 and 8. Weights were stabilized and did not fluctuate significantly during examination, no signs of stress were present to the animals. General anesthesia was administered to Sprague–Dawley rats, using methoxyfluorane for all surgical procedures. All the animals were administered with Buprenorphine SR LAB to release the pain stress caused by the surgery. Two one cm midsagittal incisions were made on the dorsa, and two subcutaneous pockets were created with hemostats via blunt dissection on each side of the incision (Figure 1). Discs with different coatings were randomized per animal by a separate examiner and surgeon was blinded to the identity of the discs. Four discs were implanted into each rat, each disc from a separate group. Once discs were inserted, sites were closed with staples and swabbed with iodine at incisions lines. A total of 13 rats had four discs implanted subcutaneously.

In-vitro Fluorescence Imaging

In vitro Fluorescent images were taken at 0,2,4,8 weeks. All fluorescent images were captured with CRi Maestro In-vivo spectral imaging system (Cambridge Research & Instrumentation, US) (Woburn, MA) (Figure 1). At each time point except week 0, four animals were euthanized using CO₂, once animal was euthanized two midsagittal incisions were made in similar area as previous surgery. Scaffolds were retrieved with the surrounding tissue (about 4 mm thick tissue around the scaffold was retrieved with the scaffold) and immediately soaked into 10 % neutral-buffered formalin. Discs were immediately placed in dark container so that fluorescence marker would not be altered by ambient light. At 2w, 4w and 8w, residual peptides within the HA scaffolds were measured with Maestro imaging system (Figure 1). There were 4 scaffolds for each treatment group at 2-week and 4-week time points, and 5 scaffolds/treatment group for 8-week time point. In total, there were 52 scaffolds and 13 rats.

Aim 2: Osteoinductive potential of DBM in Combination with E7

Sample preparation

In this study, Demineralized Bone Matrix Allograft (DBM) was procured from the Musculoskeletal Transplant Foundation (Edison, NJ). All samples provided to the surgical and evaluation team were coded to blind the reviewers to the tissue bank source as well as donor age and sex. Four different groups of DBM were tested; Active DBM (positive control) where active protein factors were present on the bone matrix from the normal tissue processing from the tissue bank. All tissue banks follow a general system that involves cleaning, defatting, and disinfecting cortical bone; grinding the defatted bone to particle sizes between 400 and 1000 mm; demineralizing the bone particles in dilute hydrochloric acid solutions, resulting in a residual calcium content of <8% per the American Association of Tissue Banks standards; and freeze-

drying the final product⁴⁶. Active DBM from the same lot was heated for twenty-four hours at 105°C to inactivate any biologically active protein factors present and served as Inactive DBM (negative control). E7HA7 was conjugated to both Inactive and active DBM matrix. Particle size was kept between 400-1000 microns, which is the typical size bone graft used for periodontal grafting. Capsules were filled with 20mg of active or inactive DBM with/without E7 peptides. Capsules were used to facilitate implantation and help localized the bone graft and prevent displacement in-situ. All samples were prepared under aseptic conditions and were stored at room temperature until samples were ready for implantation.

Experimental Design

The second part of the study was conducted under a protocol approved by the Institutional Animal Care and Use Committee at Virginia Commonwealth University. Sixteen 8-week-old nude athymic mice were divided into four groups: Active DBM (aDBM), Active DBM-E7 (aDBM-E7), Inactive DBM (iDBM), and Active DBM-E7 (iDBM-E7).

Implantation Protocol

An ectopic bone formation model was used to test the bioactivity of E7HA7 and the enhancement of osteoinductivity when combined with demineralized bone matrix. Athymic nude mice were anesthetized by inhalation of 5% isoflurane gas. A 1cm incision along gastrocnemius muscle was made and a longitudinal split with blunt dissection was created per leg. One gelatin 20mg capsule containing a variation of DBM was inserted into the muscle pouch and was closed with a wound clip (N=2/animal) (Figure 3). 8 implants were placed in each group with a total of 16 animals.

The mice were housed in appropriate conditions based on their immunocompromised status and were given food and water ad libitum for 35 days. This time period was chosen based

on previous experiments demonstrating that 35 days was sufficient time for osteoinductive activity to take place in this animal model. Animals were sacrificed at 35 days using carbon dioxide asphyxiation. The hind limbs were disarticulated and immediately placed into 10% formalin solution for future histological and morphometric assessment.

Morphometric Analysis

The ability of the samples to induce new bone were quantitatively analyzed by two separate blinded examiners using Bruker Skyscan 1173 MicroCT (Billerica, MA) (Figure 3). Each disarticulated hind leg was placed inside a plastic test tube fitted with cotton gauze to stabilize the leg from moving during imaging. The plastic test tube was placed on the platform in the machine and imaged. Once raw images were created, a superior and inferior threshold was made for each image to exclude any areas that could have bone fragments or noise from disarticulation. The examiner went through each cross section of each microCT slice, a region of interest was made around the long bones of the leg to eliminate to subtract the region of interest to determine the amount of new bone formation in each sample (Figure 4, Figure 5, Figure 6, Figure 7). Similar imaging parameters were selected for each sample and new bone formation was determined by new bone volume formation in mm³.

Histomorphometric analysis

Samples were commercially processed (Histion, Everett, WA, USA). Femurs were embedded in methyl methacrylate, and one ground section from each specimen was stained with Hematoxylin and Eosin staining. Sections were imaged with an AxioCam MRc5 camera and Axio Observer Z.1 and analyzed using ZEN 2012 Blue Edition software (Carl Zeiss Microscopy, Oberkochen, Germany).

Statistical analyses

Part 1

The study is a two-way design (four treatments and 4 time periods), with animals observed across time. This within-animal dependence is taken into account in the analysis. The interventions are compared using a repeated-measures mixed-model two-way ANOVA. Fluorescence is severely skewed and so the log-transformed values are used for analyses. The least-squared mean estimated values for each group are back-transformed to the original scale, yielding geometric mean values. Differences between treatments are identified at each week using pre-specified contrasts. All analyses were performed using SAS software (JMP pro version 13.2, SAS version 9.4, SAS Institute Inc., Cary NC).

Part 2

The study is a two-way design (Active vs Inactive and E7HA7 yes vs no), with the interventions assigned to either the left or right leg of the animal. This within-animal dependence is taken into account in the analysis. The interventions are compared using a repeated-measures mixed-model two-way ANOVA. The bone volume (in mm³) is severely skewed and so the log-transformed values are used for analyses. The least-squared mean estimated values for each group are back-transformed to the original scale, yielding geometric mean values. Differences between the four groups are identified by Tukey's honestly significantly different multiple comparison procedure (at alpha = 0.05).

Results

Weights among the animals remained stable throughout the experiment. No animal deaths were observed throughout the experiment, and all animals tolerated the procedures well.

Aim 1: Retention of E-7 Peptide on HA discs

Qualitatively, at week 0 discs coated with E7-HA2-FITC had the strongest fluorescence signal, especially on the perimeter of the discs. Qualitatively, E7-HA7-FITC groups had the highest fluorescence intensity at 2,4, and 8 weeks. Interestingly, fluorescence was mainly noted on perimeter of discs. The fluorescence intensity of each group at the four time periods is shown in (Figure 8). Fluorescence values are strongly skewed with higher variability occurring at brighter intensity. Based on the skewed intensity a two-way ANOVA analysis analyzed the log-transformed values to equalize the variability within groups. The back-transformed values for each group are summarized in (Table 1). In the peptide releasing study, all three peptide groups had statistically stronger fluorescence signals at all the time points compared to control discs. E7HA7 coated scaffolds had stronger fluorescent signals at all three time points compared to other groups, indicating a longer retention and stronger affinity for HA scaffolds. E7HA7 showed slower peptide release from scaffolds in comparison to other groups, being statistically significant at week 2 compared to E7, and to E7HA2 at week 4 and week 8(Figure 8,Figure 9).

Aim 2: The osteogenic potential of bone graft material combined with E7HA peptide

New Bone Volume Formation

The median values for new bone formation are: iDBM=0.041mm³, iDBM-E7=0.071mm³, aDBM=0.138mm³, and aDBM-E7=0.192mm³ (Figure 10). As is typical with volume measurements, the values were skewed. The two-way repeated-measures ANOVA was performed on the log-transformed bone levels. There was a significant difference between the

active and inactive groups ($P=0.008$), but no significant difference between the E7 vs E7HA7 groups ($P=0.187$). Although new bone formation was greater in aDBM-E7, significant difference was only found when compared to the iDBM group (Table 2). When comparing controls, aDBM vs iDBM, aDBM had a greater bone formation than iDBM, however the difference was not statistically significant. The addition of E7HA7 increased the bone volume 1.48 times ($P=0.48$) in the inactive DBM group and 1.98 times ($P=0.23$) in the active DBM group, but the additive benefit did not reach statistical significance.

The results of the multiple comparison procedure are shown in Table 3. As mentioned earlier, the only statistically significant difference of new bone formation was between aDBM-E7 vs. iDBM, where aDBM had 5.6 times more new bone formation present ($p = 0.03$). It is interesting to point out that, if we only compare the active DBM to inactive DBM (without E7HA7 coating), although more bone formation (2.82 times as high) was seen in the active DBM group, the difference was not statistically significant ($P=0.27$).

Histological Observations

All photomicrographs were screened, and one representative sample was chosen from each group to be included for qualitative assessment. Photomicrographs of Inactive samples showed DBM particles, surrounded by a combination of connective tissue, adipose tissue, and muscles tissues. The inactive samples did not show any new bone formation within the samples. No new bone formation was demonstrated by a homogeneous color of bone particle with the absence of osteoclasts, osteoblasts, and hematopoietic cells surrounding the periphery of the graft or within lacunae. No inflammatory cells were noted in the inactive samples surrounding bone particles (Figure 11). A general trend noticed in active samples was fewer DBM particles

present, possibly indicating that heat treatment of the bone graft could have led to increased resorption of the DBM particles

Active groups demonstrated DBM particles, surrounded by a combination of connective tissue, adipose tissue, and muscles tissues. When comparing both active and inactive samples there was more presence of bone graft in the active samples, indicating less resorption of the bone graft. Although a larger quantity of bone graft was present in active samples, there was minimal to no new bone formation present seen by uniform color of the residual graft material and lack of bone marrow, immature bone, and hematopoietic cells (Figure 12).

The addition of E7 to inactive groups showed similar morphology to inactive groups, however the addition of E7 showed less resorption of graft materials and the presence of a greater number of particles in comparison to iDBM samples by themselves (Figure 13). More robust osteoinduction was present in active samples in combination with E7 peptide. Presence of Ossicles (bone-like tissue surrounding an area of bone marrow-like tissue) was present in aDBM-E7 samples (Figure 14,

Figure 15). Ossicles are indicative of mature bone formation. In addition, presence of osteocytes and hematopoietic cells was present in aDBM-E7 samples. Since limited new bone formation was present in the aDBM alone, and more mature bone formation was present with the addition of E7 peptide in several samples is a possible indication of osteoinductive enhancement of the DBM.

Discussion

Numerous bone substitute materials are used for periodontal regeneration, each one with their positive and negative attributes. Limitations of synthetic HA are that the alloplastic material has good osteoconductive properties but lacks the osteoinductive properties. However, surface functionalization of HA through the addition of osteoinductive molecules can enhance the regenerative outcomes.

The success in periodontal and bone regenerative procedures is still highly dependent on the defect morphology and regenerative potential of the patient. Previous studies have shown that there are numerous modalities for enhancing osteoinductivity of bone material, such as the delivery of stem cells, platelet rich plasma, and recombinant proteins (Platelet Derived Growth Factor BB and bone morphogenic proteins). Although there are benefits to adding various enhancing products, the molecules are passively adsorbed to the surface and have low binding capacity to the grafting material, limiting effective release control kinetics. To enhance bone binding and release kinetics various mechanisms mimicking the endogenous bone matrix proteins, such as GLA protein, osteonectin and bone sialoprotein, have been identified. A bone binding motif consisting of negatively charged amino acids such a glutamic acid is one of them. One of the first groups to identify the affinity of glutamic acid to HA crystals was Fujisawa, who showed that through degradation of osteonectin, the residual binding residues were rich in glutamic acid⁴⁵. In later studies, Fujisawa compared the binding of osteoblastic cells to HA coated BSP, osteonectin, bovine serum albumin and Glu7-Pro-Arg-Gly-Asp- Thr (E7TPRGDT). E7TPRGDT was used because it contained both a putative hydroxyapatite- binding sequence and the RGD sequence, a cell binding motif. E7TPRGDT being 1/50 the size of BSP had similar

ability to recruit osteoblastic cells as BSP, and the dissociation constant was 500x times greater than that of BSP.

The Culpepper group has also demonstrated the enhanced coupling of polyglutamic acids to bioactive peptides for enhanced retention and controlled release in vitro and in vivo models. DGEA (Asp-Gly-Glu-Ala), a collagen derived peptide were synthesized with variable length polyglutamate chains (diglutamate (E2), tetraglutamate (E4), and heptaglutamate (E7) and adsorbed on to HA discs and allograft particles and retention was determined³⁶. In all mediums and assays E7>E4>E2 had increased peptide loading and retention after 5 days³⁶. The bound peptide released ranged from in E7-DGEA was <10% after 5 days in Saline agitation and ~35% in serum containing media, while DGEA alone was nearly 90-100% released in both medias after a 5 day period³⁶. In similar medias, improved retention was noted on HA discs vs Allograft, however different binding substrates (HA discs vs allograft particle) was used.

In Polini's study comparing release kinetics of E7 (polyglutamate), Osteocalcin (OCN), and salivary statherin (N7) adsorbed to similar HA discs used in our study, the results were comparable to release kinetics present in our study. Overall E7 had the greatest retention compared to OCN and N7. When these retentive molecules were tested on their own at a 1-month time period, 75% of E7, 30% of OCN, and 25% of N7 was still retentive on the HA scaffolds⁴⁷. When E7 was combined with osteogenic molecules such as Osteogenic Growth peptide (OGN) and Bone morphogenic Protein -7 (BMP-7) the addition of osteogenic molecules did not affect peptide retention and at a 1-month time point nearly 60% of the peptide was retained. The combination of an osteogenic molecules with E7 did not affect the binding and releasing properties of E7.

Similarly, in our study when comparing varying polyglutamate chains, the E7HA7 had the greatest retention on discs over an 8-week period. E7HA7 showed slower peptide release from being statistically significant at week 2 compared to E7, and to E7HA2 at week 4 and week 8. Culpepper showed that DGEA alone had quickest release, nearly 100% released by 5 days and E2 had quicker releasing at all time points in comparison to E7. In our current experiment over an 8-week period although E7HA7 had greatest retention, interestingly E7 alone vs E7HA2 had greater retention at 4 and 8-week time points. However, this was not statistically significant. In addition, when examining the release curves of the various groups it is evident that at the 1-week time point E7 and E7HA2 were nearly one hundred percent released, where E7HA7 still has approximately 50% of peptide bound to the HA discs. Reasons for greater retention could be due to uneven distribution of peptide along the HA surfaces, where more would accumulate on the edge of the discs as opposed to the center of the discs. Greater accumulation along the edge of the discs could be speculated to having a greater surface roughness and increased surface area for binding for the bioactive peptides within the study. In addition to greater accumulation on the edges, the stronger fluorescence intensity seen from the edge of the discs could also wash out the fluorescent intensity that may be present on the middle of the discs. Quantification of peptide release in our study was difficult due determine to a different model used in comparison to the Culpepper studies, where they used serum containing media or saline media, our studies used a subcutaneous environment of rats making it difficult to have a standard to compare direct release.

In another study by the Culpepper group they examined the effects of Heptaglutamate domain coupled with DGEA peptide on HA discs and HA discs coupled with electrospun scaffolds⁴⁸. Similarly, in their studies, in a subcutaneous model DGEA coupled with

Heptaglutamate had the greatest retention on HA discs coupled with and without electrospun scaffolds, in comparison to DGEA alone. The results indicate that surface modification of bony substrates with bioactive peptides can serve as a vehicle for long term release of regenerative molecules. Modulating the release of the bioactive peptides, E7 has the potential to recruit autologous bone marrow derived, periodontal, and pulpal stem cells to the periodontal defect for regeneration.

Numerous experiments including ours have shown increased retention of peptides to both hydroxyapatite and allograft materials through ionic coupling of polyglutamate domains to endogenous bone matrix proteins. Demineralized allograft materials, another popular graft for regeneration due to its exposed osteoinductive proteins on the surface have been shown to be successful in periodontal regeneration. However, the osteoinduction potential often varies among various demineralized allografts due to inactive proteins within the graft, insufficient quantities, processing methods, residual calcium levels, age of donor, and medical status. To our knowledge, the addition of modified E7 (EPLQLKM) peptide to DBM, is one of the first in-vivo experiments to test the additive effects to osteoinductivity of E7 to DBM.

The additive effect of the E7HA7 to DBM increased bone volume about 1.5 times in the inactive DBM and about two times in the active DBM. Although the osteoinductive enhancement of E7 is not statistically significant, it is suggestive of an enhancement of the osteoinductive potential. The lack of statistical significance for new bone formation could be due to several reasons. As shown initially by Fujisawa, when heptaglutamate was coupled with PRGDT, there was a positive correlation with peptide binding with calcium ions, and negative correlation with phosphate ions, measured through fluorometry⁴⁵. Based on the AATB, the DBM used in this experiment has less than 8% residual calcium present according to the manufacturer

website which suggests that only a small percentage of E7 heptaglutamate would have been bound to the graft. Additionally Culpepper, demonstrated that, with electrospun polycaprolactone (PCL) scaffolds compared to HA discs under constant wash for 7 days, PCL alone was insufficient for retaining E7-DGEA, and that HA is needed to facilitate binding⁴⁸.

The intent of demineralization of allograft is to expose the proteoglycan/collagen matrix and protein factors such as bone morphogenic proteins. Zhang, showed that FDBA demineralized with hydrochloric acid, depending on the demineralization time the residual calcium by weight can drop from ~32% to ~1% if demineralized up to 300 minutes²². In addition, Zhang demonstrated that osteoinductivity of DBM can also vary based on particle size. The particle size with most osteoinductive potential ranged from 500-710 microns, whereas particles less than 250 microns had significantly reduced osteoinductive potential compared to other particle sizes²². Demineralized bone was used in this intramuscular model so that new calcification/osteogenesis could be quantified through micro-CT imaging.

The weak enhancement of E7 to the osteoinductive potential of DBM and range of bone volume formations can be explained due to several reasons. Based on histology from our study it was evident that very weak new bone formation and osteoinduction was present in the active DBM group. According to Schwartz et al, the variability and lack of osteoinductivity could be due to processing methods of the tissue bank, insufficient time for the new bone formation to occur, batch used in the experiment is not osteoinductive²¹. The particular batch from our study could not have been as inductive as other batches, Schwartz found that 18% of the batches had no osteoinductivity, and 40% had only moderate inductivity²⁰. Lastly, insufficient time could have resulted in less bone formation. In Schwartz 1996 study bone formation was assessed at day 28 and day 56, where a larger amount of new bone formation was evident at day 56 in

comparison to day 28. Increased bone volume formation at a later time point was due to a less robust osteoinductive effect at an earlier time point²¹. There is a possibility that a longer time could have resulted in more new and mature bone formation for the active group with and without E7 with a longer incubation time. Although hardly any new and mature bone formation was seen in aDBM group, the combination of E7 peptide, did enhance formation of new and mature bone. The presence of new and mature bone formation presents in several samples only in the aDBM-E7 group, indicate that there is an enhancement of osteoinductivity with E7 peptide.

The variability in particle size could account for the broad range of volumetric measurements among groups. Although uniform amount of bone was used among each group, the small variance in particle size could affect osteogenesis and osteoinduction. The weak osteoinductive enhancement of E7 could also be due to the residual calcium particles left over within the graft. Since demineralized bone was used, the low concentration of calcium within the graft could account for a weak binding affinity of E7 peptide to the demineralized bone, which would affect osteoinductive enhancement. Although a high binding affinity was shown for HA discs and E7HA7, no attempts at this time have been made to quantify affinity or retention of E7HA7 on demineralized bone. Additionally one of the difficulties in mesenchymal stem cell homing is the low efficiency and engraftment of endogenous mesenchymal cells²⁹. As previously shown, Bone Marrow Derived Mesenchymal Cells have the ability to differentiate into dental progenitor cells, the highest engraftment of mesenchymal cells was seen in pulpal and periodontal tissues as opposed to lung, liver, and adipose tissue³². The reason for higher engraftment was due to continuous remodeling of periodontal tissue, a connective pathway between the bone marrow cavity and periodontium of the mandible, and higher expression of

SDF-1 protein in dental mesenchymal tissues³². Therefore, based on location of particulate placement as shown in other studies, it may be difficult to home the necessary osteoblasts needed for osteogenesis.

There are several limitations that apply to this study. In both portions of the experiment a larger number of samples within each group could have been used yielding a stronger result. In the second portion of the study, affinity and retention of DBM particulate in combination with E7 BMSC affinity peptide could have been examined in-vitro to determine binding capabilities and affinities. Additionally, a mineralized bone graft could have been compared to a demineralized bone graft to see if there was an additive benefit of E7 to the bone graft. Although there are limitations to the current model used to determine the benefit of E7 for osteogenesis, future studies will use periodontal defects to determine the ability of E7 to home in mesenchymal stem cells.

Conclusion

Conjugation of E7 to polyglutamate bone binding domain showed long –lasting releasing kinetics from hydroxyapatite scaffolds. Based on the results, we can conclude that E7HA7 promotes a stronger affinity to the Hydroxyapatite scaffold, with improved retention and controlled release. The conjugation of E7HA7 peptide to inactive and active DBM slightly enhanced the osteoinductivity potential of both allografts. Thus, E7HA7 may be used to enhance bone regeneration for guided tissue regeneration procedures in the future, however further studies need to be conducted.

Appendices

Appendix 1: Conflict of interest Disclosure

The authors have no known conflicts of interest associated with this publication, and there has been no significant financial support for this work that could have influenced this outcome

Bibliography

1. Eke PI, Dye BA, Wei L, Thornton-Evans GO, Genco RJ, CDC Periodontal Disease Surveillance workgroup: James Beck (University of North Carolina, Chapel Hill, USA), Gordon Douglass (Past President, American Academy of Periodontology), Roy Page (University of Washin. Prevalence of Periodontitis in Adults in the United States: 2009 and 2010. *J Dent Res.* 2012 Oct 30;91(10):914–20.
2. Becker W, Berg L, Becker BE. Untreated periodontal disease: a longitudinal study. *J Periodontol.* 1979 May;50(5):234–44.
3. Caffesse RG, Sweeney PL, Smith BA. Scaling and root planing with and without periodontal flap surgery. *J Clin Periodontol.* 1986 Mar;13(3):205–10.
4. Harrel SK, Nunn ME. Longitudinal comparison of the periodontal status of patients with moderate to severe periodontal disease receiving no treatment, non-surgical treatment, and surgical treatment utilizing individual sites for analysis. *J Periodontol.* 2001 Nov;72(11):1509–19.
5. Kaldahl WB, Kalkwarf KL, Patil KD, Molvar MP, Dyer JK. Long-Term Evaluation of Periodontal Therapy: II. Incidence of Sites Breaking Down. *J Periodontol.* 1996 Feb;67(2):103–8.
6. Melcher AH. On the Repair Potential of Periodontal Tissues. *J Periodontol.* 1976 May;47(5):256–60.
7. Melcher AH, McCulloch CA, Cheong T, Nemeth E, Shiga A. Cells from bone synthesize cementum-like and bone-like tissue in vitro and may migrate into periodontal ligament in vivo. *J Periodontal Res.* 1987 May;22(3):246–7.
8. Rios HF, Lin Z, Oh B, Park CH, Giannobile W V. Cell- and Gene-Based Therapeutic Strategies for Periodontal Regenerative Medicine. *J Periodontol.* 2011 Sep;82(9):1223–37.

9. Nyman S, Gottlow J, Karring T, Lindhe J. The regenerative potential of the periodontal ligament. An experimental study in the monkey. *J Clin Periodontol.* 1982 May;9(3):257–65.
10. Gottlow J, Nyman S, Karring T, Lindhe J. New attachment formation as the result of controlled tissue regeneration. *J Clin Periodontol.* 1984 Sep;11(8):494–503.
11. Wikesjö UME, Crigger M, Nilvéus R, Selvig KA. Early Healing Events at the Dentin-Connective Tissue Interface. Light and Transmission Electron Microscopy Observations. *J Periodontol.* 1991 Jan;62(1):5–14.
12. Iglhaut J, Aukhil I, Simpson DM, Johnston MC, Koch G. Progenitor cell kinetics during guided tissue regeneration in experimental periodontal wounds. *J Periodontal Res.* 1988 Mar;23(2):107–17.
13. Ranganath SH, Levy O, Inamdar MS, Ksarp JM. Harnessing the mesenchymal stem cell secretome for the treatment of cardiovascular disease. *Cell Stem Cell.* 2012 Mar 2;10(3):244–58.
14. Wang H-L, Boyapati L. PASS principles for predictable bone regeneration. *Implant Dent.* 2006 Mar;15(1):8–17.
15. Froum SJ, Ortiz M, Witkin RT, Thaler R, Scopp IW, Stahl SS. Osseous Autografts: III. Comparison of Osseous Coagulum-Bone Blend Implants with Open Curettage. *J Periodontol.* 1976 May;47(5):287–94.
16. Cortellini P, Prato GP, Tonetti MS. Periodontal Regeneration of Human Infrabony Defects. II. Re-Entry Procedures and Bone Measures. *J Periodontol.* 1993 Apr;64(4):261–8.
17. Murphy KG, Gunsolley JC. Guided tissue regeneration for the treatment of periodontal

- intrabony and furcation defects. A systematic review. *Ann Periodontol.* 2003 Dec;8(1):266–302.
18. Urist MR, Strates BS. The classic: Bone morphogenetic protein. *Clin Orthop Relat Res.* 2009 Dec 1;467(12):3051–62.
 19. Shigeyama Y, D’Errico JA, Stone R, Somerman MJ. Commercially-prepared allograft material has biological activity in vitro. *J Periodontol.* 1995 Jun;66(6):478–87.
 20. Schwartz Z, Somers A, Mellonig JT, Carnes DL, Dean DD, Cochran DL, et al. Ability of Commercial Demineralized Freeze-Dried Bone Allograft to Induce New Bone Formation Is Dependent on Donor Age But Not Gender. *J Periodontol.* 1998 Apr;69(4):470–8.
 21. Schwartz Z, Mellonig JT, Carnes DL, Fontaine JD La, Cochran DL, Dean DD, et al. Ability of Commercial Demineralized Freeze-Dried Bone Allograft to Induce New Bone Formation. *J Periodontol.* 1996 Sep;67(9):918–26.
 22. Zhang M, Powers RM, Wolfenbarger L. Effect(s) of the Demineralization Process on the Osteoinductivity of Demineralized Bone Matrix. *J Periodontol.* 1997 Nov;68(11):1085–92.
 23. Mellonig JT, Bowers GM, Cotton WR. Comparison of Bone Graft Materials: Part II. New Bone Formation With Autografts and Allografts: A Histological Evaluation. *J Periodontol.* 1981 Jun;52(6):297–302.
 24. Laurell L, Gottlow J, Zybutz M, Persson R. Treatment of Intrabony Defects by Different Surgical Procedures. A Literature Review. *J Periodontol.* 1998 Mar;69(3):303–13.
 25. Rummelhart JM, Mellonig JT, Gray JL, Towle HJ. A comparison of freeze-dried bone allograft and demineralized freeze-dried bone allograft in human periodontal osseous defects. *J Periodontol.* 1989 Dec;60(12):655–63.

26. Reynolds MA, Aichelmann-Reidy ME, Branch-Mays GL, Gunsolley JC. The Efficacy of Bone Replacement Grafts in the Treatment of Periodontal Osseous Defects. A Systematic Review. *Ann Periodontol.* 2003;8(1):227–65.
27. Lin Z, Rios HF, Cochran DL. Emerging regenerative approaches for periodontal reconstruction: a systematic review from the AAP Regeneration Workshop. *J Periodontol.* 2015 Feb;86(2 Suppl):S134-52.
28. Cochran DL, Cobb CM, Bashutski JD, Chun Y-HP, Lin Z, Mandelaris GA, et al. Emerging regenerative approaches for periodontal reconstruction: a consensus report from the AAP Regeneration Workshop. *J Periodontol.* 2015 Feb;86(2 Suppl):S153-6.
29. Karp JM, Leng Teo GS. Mesenchymal stem cell homing: the devil is in the details. *Cell Stem Cell.* 2009 Mar 6;4(3):206–16.
30. Hynes K, Menicanin D, Gronthos S, Bartold PM. Clinical utility of stem cells for periodontal regeneration. *Periodontol 2000.* 2012 Jun;59(1):203–27.
31. Yang Y, Rossi FM V, Putnins EE. Periodontal regeneration using engineered bone marrow mesenchymal stromal cells. *Biomaterials.* 2010 Nov;31(33):8574–82.
32. Zhou J, Shi S, Shi Y, Xie H, Chen L, He Y, et al. Role of bone marrow-derived progenitor cells in the maintenance and regeneration of dental mesenchymal tissues. *J Cell Physiol.* 2011 Aug;226(8):2081–90.
33. Discher DE, Mooney DJ, Zandstra PW. Growth factors, matrices, and forces combine and control stem cells. *Science.* 2009 Jun 26;324(5935):1673–7.
34. Shao Z, Zhang X, Pi Y, Wang X, Jia Z, Zhu J, et al. Polycaprolactone electrospun mesh conjugated with an MSC affinity peptide for MSC homing in vivo. *Biomaterials.* 2012;33(12):3375–87.

35. Huang H, Zhang X, Hu X, Shao Z, Zhu J, Dai L, et al. A functional biphasic biomaterial homing mesenchymal stem cells for in vivo cartilage regeneration. *Biomaterials*. 2014 Dec;35(36):9608–19.
36. Culpepper BK, Webb WM, Bonvallet PP, Bellis SL. Tunable delivery of bioactive peptides from hydroxyapatite biomaterials and allograft bone using variable-length polyglutamate domains. *J Biomed Mater Res A*. 2014 Apr;102(4):1008–16.
37. Bessa PC, Casal M, Reis RL. Bone morphogenetic proteins in tissue engineering: the road from laboratory to clinic, part II (BMP delivery). *J Tissue Eng Regen Med*. 2(2–3):81–96.
38. Luong LN, Hong SI, Patel RJ, Outslay ME, Kohn DH. Spatial control of protein within biomimetically nucleated mineral. *Biomaterials*. 2006 Mar;27(7):1175–86.
39. Guan M, Yao W, Liu R, Lam KS, Nolte J, Jia J, et al. Directing mesenchymal stem cells to bone to augment bone formation and increase bone mass. *Nat Med*. 2012 Feb 5;18(3):456–62.
40. Murphy MB, Hartgerink JD, Goepferich A, Mikos AG. Synthesis and in vitro hydroxyapatite binding of peptides conjugated to calcium-binding moieties. *Biomacromolecules*. 2007 Jul;8(7):2237–43.
41. Price PA, Otsuka AA, Poser JW, Kristaponis J, Raman N. Characterization of a gamma-carboxyglutamic acid-containing protein from bone. *Proc Natl Acad Sci U S A*. 1976 May;73(5):1447–51.
42. Oldberg A, Franzén A, Heinegård D. The primary structure of a cell-binding bone sialoprotein. *J Biol Chem*. 1988 Dec 25;263(36):19430–2.
43. Bolander ME, Young MF, Fisher LW, Yamada Y, Termine JD. Osteonectin cDNA sequence reveals potential binding regions for calcium and hydroxyapatite and shows

- homologies with both a basement membrane protein (SPARC) and a serine proteinase inhibitor (ovomucoid). *Proc Natl Acad Sci U S A*. 1988 May;85(9):2919–23.
44. Gorski JP. Acidic phosphoproteins from bone matrix: a structural rationalization of their role in biomineralization. *Calcif Tissue Int*. 1992 May;50(5):391–6.
 45. Fujisawa R, Wada Y, Nodasaka Y, Kuboki Y. Acidic amino acid-rich sequences as binding sites of osteonectin to hydroxyapatite crystals. *Biochim Biophys Acta*. 1996 Jan 4;1292(1):53–60.
 46. Schwartz Z, Hyzy SL, Moore MA, Hunter SA, Ronholdt CJ, Sunwoo M, et al. Osteoinductivity of demineralized bone matrix is independent of donor bisphosphonate use. *J Bone Joint Surg Am*. 2011 Dec 21;93(24):2278–86.
 47. Polini A, Wang J, Bai H, Zhu Y, Tomsia AP, Mao C. Stable biofunctionalization of hydroxyapatite (HA) surfaces by HA-binding/osteogenic modular peptides for inducing osteogenic differentiation of mesenchymal stem cells. *Biomater Sci*. 2:1779–86.
 48. Culpepper BK, Phipps MC, Bonvallet PP, Bellis SL. Enhancement of peptide coupling to hydroxyapatite and implant osseointegration through collagen mimetic peptide modified with a polyglutamate domain. *Biomaterials*. 2010 Dec;31(36):9586–94.

Tables

Table 1. Fluorescence Intensity by Peptide coating group at each Week

Peptide Coating	Fluorescence intensity (au)		
	Geo. Mean	95% CI	
Week 0 (n=4)			
Control	9.1	2.3	35.8
E7-FITC	12,339.6 ^a	3,127.5	48,685.5
E7HA2-FITC	29,518.9 ^a	7,481.7	116,466.2
E7HA7-FITC	15,689.2 ^a	3,976.5	61,901.3
Week 2 (n=4)			
Control	2.3	0.6	9.0
E7-FITC	145.2 ^a	36.8	573.1
E7HA2-FITC	925.8 ^a	234.6	3,653.4
E7HA7-FITC	4,224.7 ^{a,b}	1,070.8	16,668.6
Week 4 (n=4)			
Control	0.7	0.2	2.9
E7-FITC	132.9 ^a	33.5	526.7
E7HA2-FITC	46.7 ^a	11.8	184.1
E7HA7-FITC	613.1 ^{a,c}	155.4	2,418.8
Week 8 (n=5)			
Control	1.8	0.5	6.0
E7-FITC	152.4 ^a	44.7	520.4
E7HA2-FITC	77.4 ^a	22.7	264.1
E7HA7-FITC	540.5 ^{a,c}	158.3	1,844.6

Notes: Least-squares mean estimated values from a repeated-measures mixed-model ANOVA were back-transformed to the original units to yield geometric means. Differences were identified by specific contrasts.

Table 2. New bone volume, by groups

		New bone volume (mm ³)		
Activity	E7HA7	Estimate *	95% CI	p-value
Inactive	no	0.034 ^a	0.015	0.077
	yes	0.050 ^{a,b}	0.022	0.114
	ratio	1.482	0.460	4.773
Active	no	0.095 ^{a,b}	0.042	0.217
	yes	0.188 ^b	0.082	0.429
	ratio	1.976	0.614	6.364

* The superscript values after the geometric mean estimate indicate group differences. Groups sharing the same superscript are not significantly different, by Tukey's HSD (P<0.05).

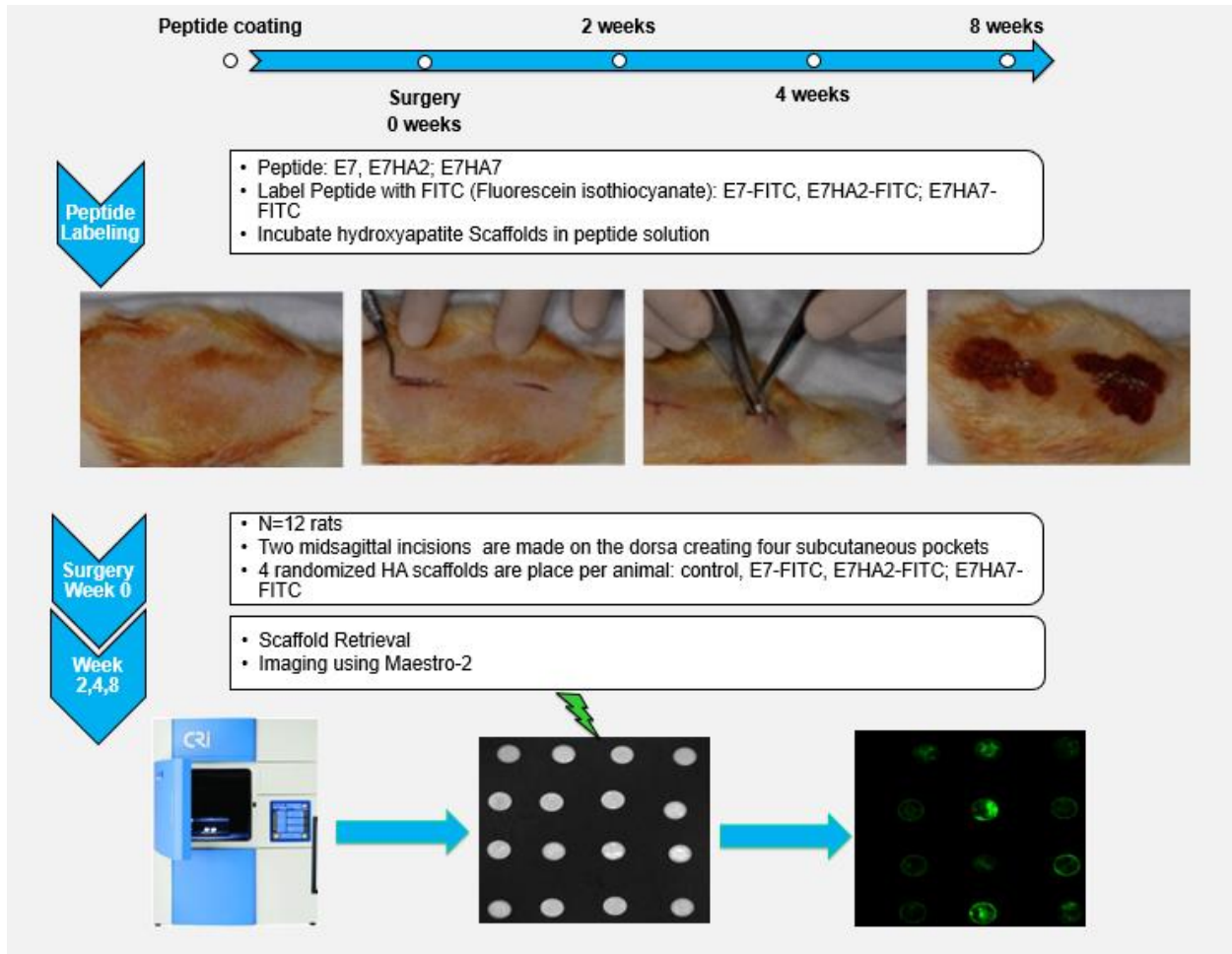
Table 3. Paired comparisons between groups

Comparison				Ratio	95% CI		Adjusted p-value
Active	no	vs.	Active yes	0.51	0.10	2.46	0.6117
Active	no	vs.	Inactive no	2.82	0.58	13.71	0.2736
Active	no	vs.	Inactive yes	1.90	0.39	9.25	0.6525
Active	yes	vs.	Inactive no	5.57	1.15	27.09	0.0312
Active	yes	vs.	Inactive yes	3.76	0.77	18.28	0.1170
Inactive	no	vs.	Inactive yes	0.67	0.14	3.28	0.8889

Note: Differences on the log-scale, when back-transformed to the original scale are interpreted as the ratio of the groups compared. Active=active DBM; inactive=inactive DBM; yes=with E7HA7 peptide; no=no E7HA7 peptide.

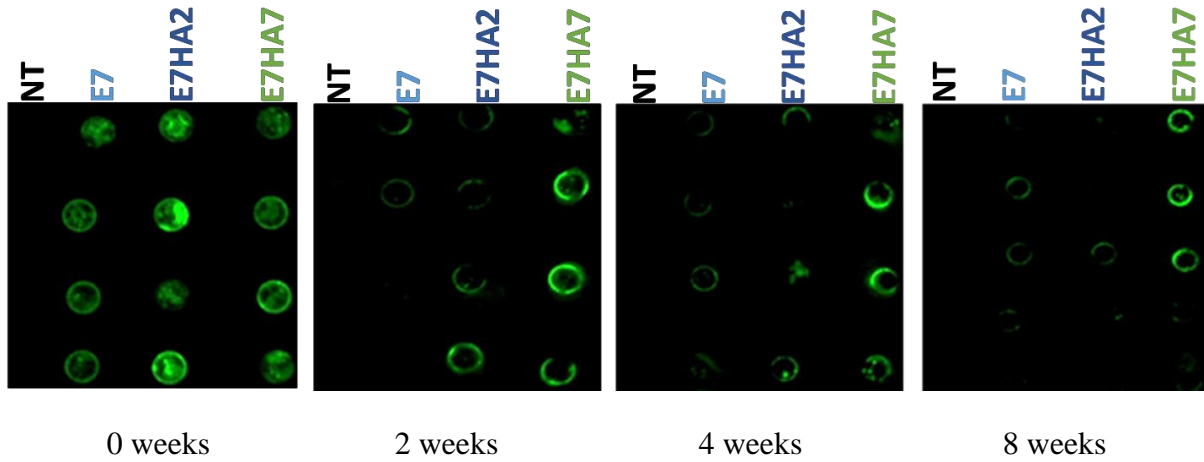
Figures

Figure 1: Disc Implantation in Animals and Fluorescent Imaging for Aim 1



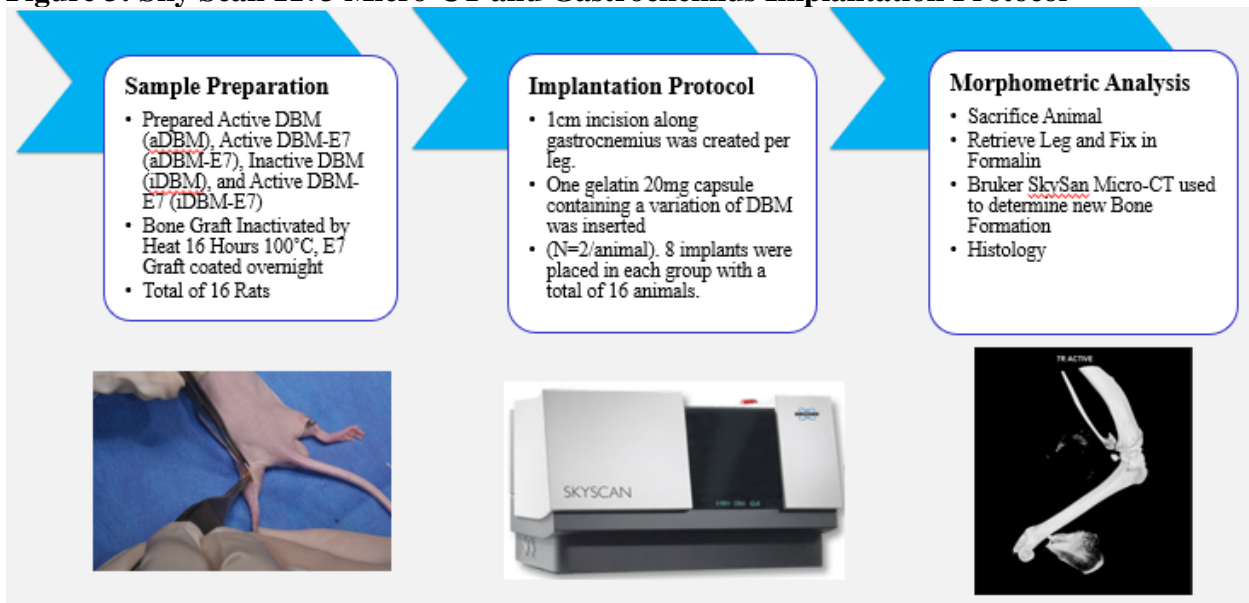
Schematic representation of subcutaneous implantation of hydroxyapatite discs and fluorescent imaging

Figure 2: In-vivo Fluorescence Readings at t 0,2,4, and 8 Weeks



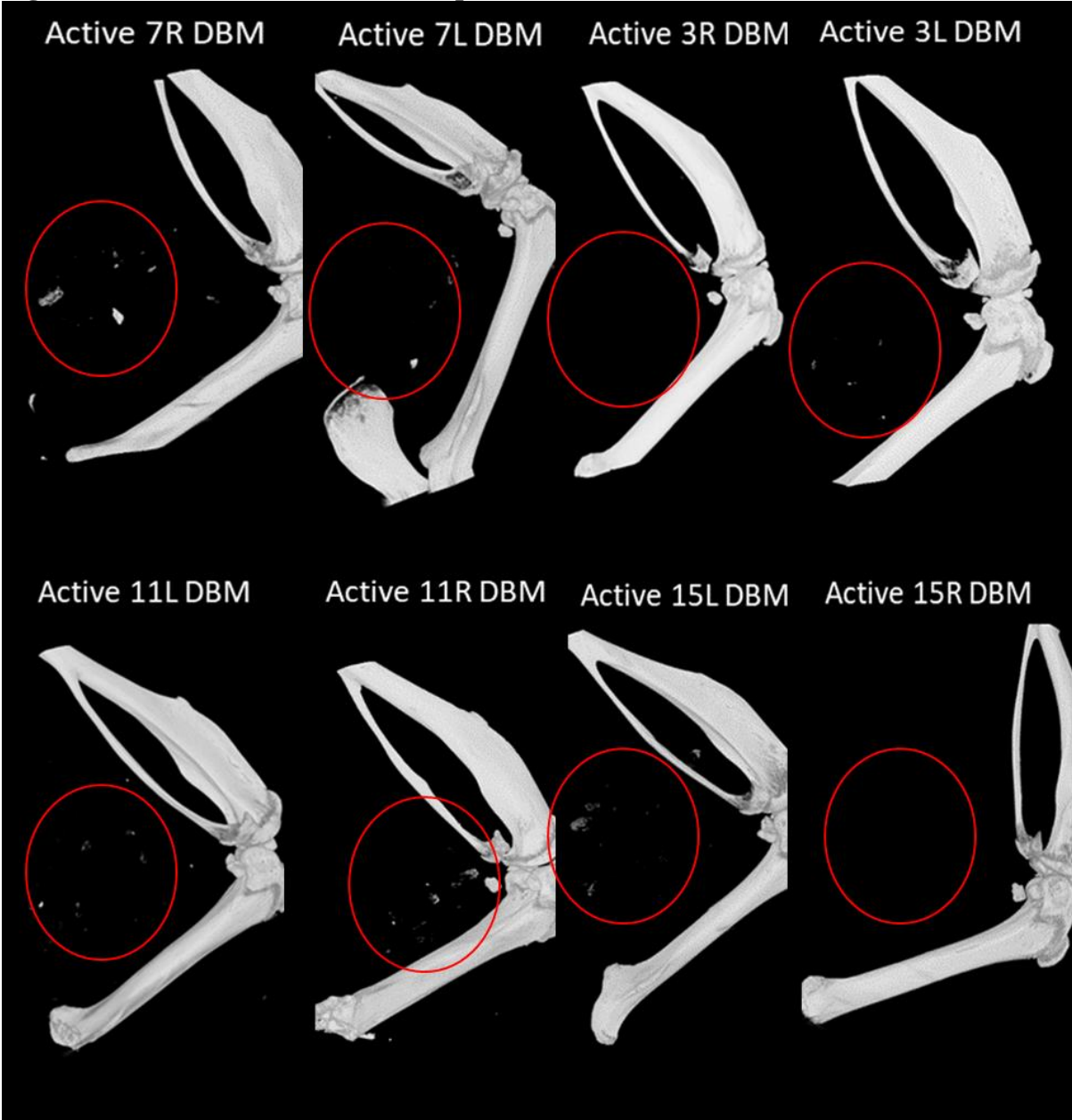
E7HA7 peptide coated scaffolds qualitatively have stronger fluorescent signals at 2,4,8 weeks indicating longer retention and stronger affinity for HA discs. Strongest fluorescence can be noted on peripheries of disks. (n=4 or 5)

Figure 3: Sky Scan 1173 Micro-CT and Gastrocnemius Implantation Protocol



Surgical Implantation of gelatin capsules containing Demineralized Bone Matrix into gastrocnemius muscle of athymic nude mice

Figure 4: Active DBM MicroCT Ectopic Bone Formation



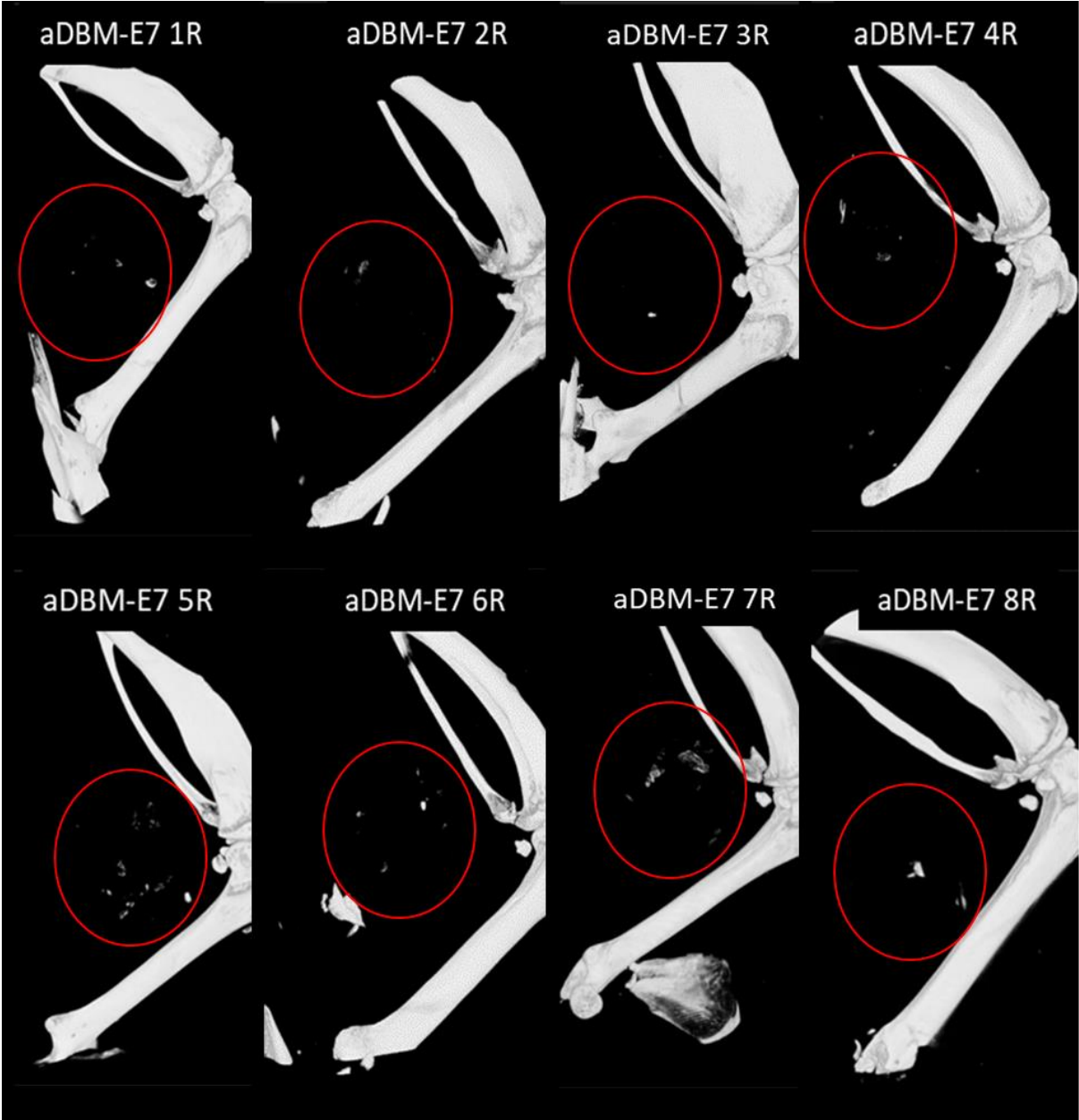
MicroCT rendering of ectopic bone formation. New bone formation can be denoted inside red circle.

Figure 5: Inactive DBM MicroCT Ectopic Bone Formation



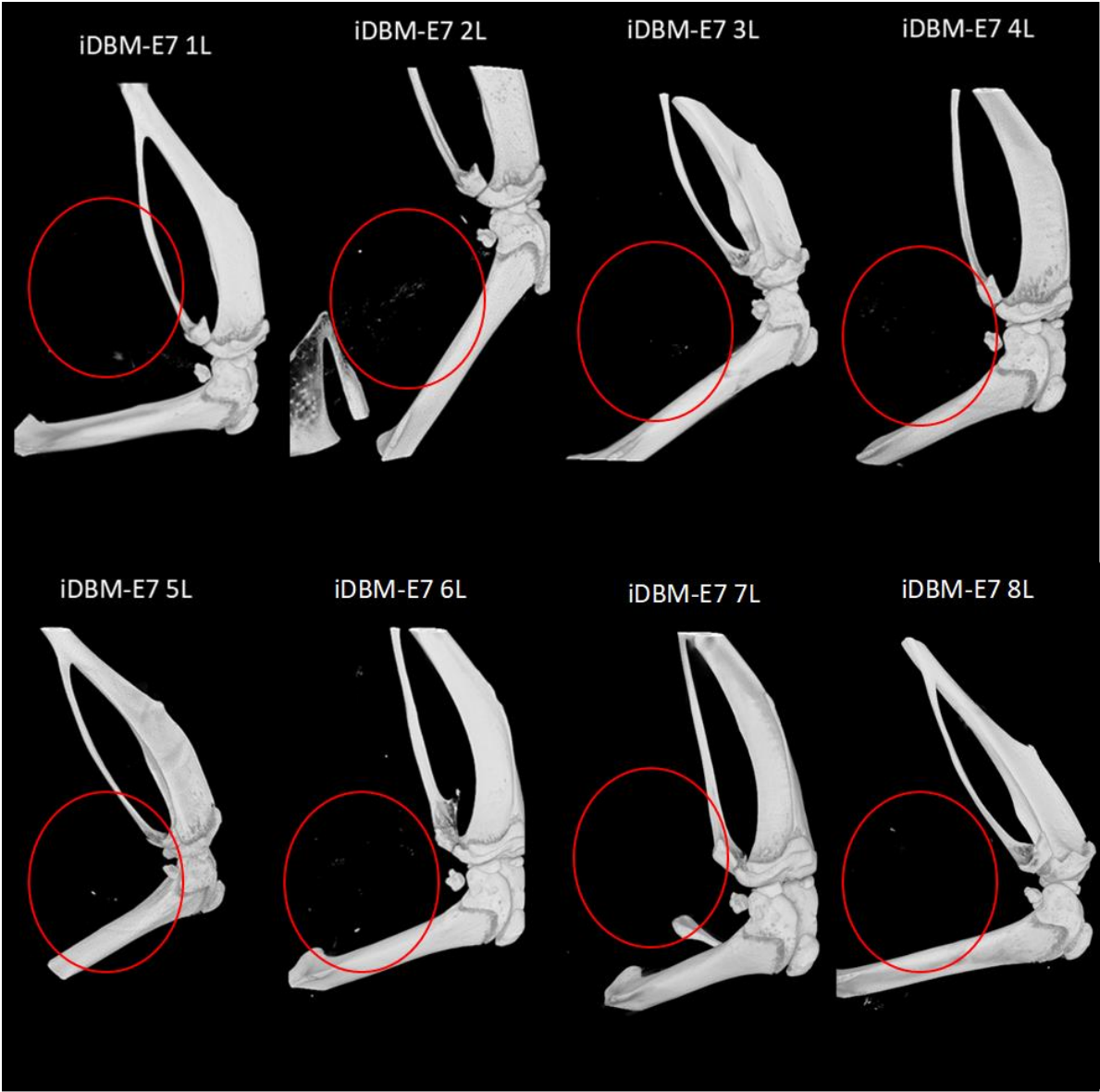
MicroCT rendering of ectopic bone formation. New bone formation can be denoted inside red circle.

Figure 6: Active DBM E7-Heptaglutamate MicroCT Ectopic Bone Formation



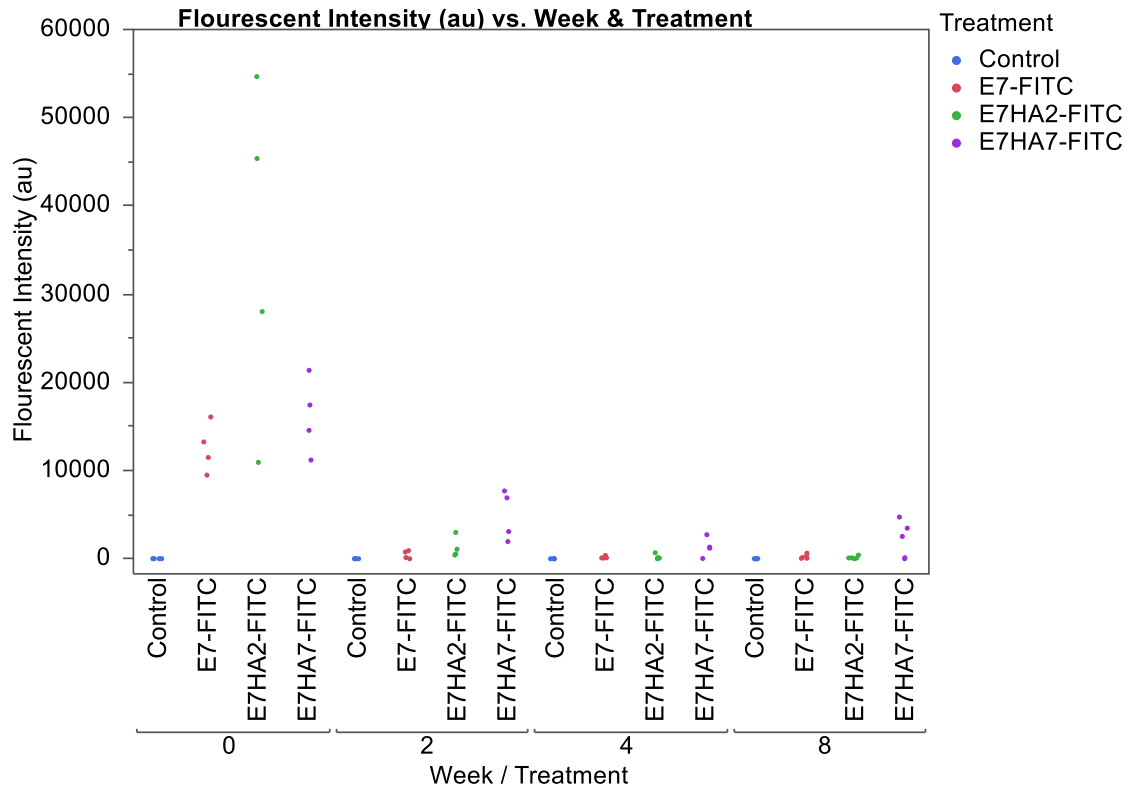
MicroCT rendering of ectopic bone formation. New bone formation can be denoted inside red circle.

Figure 7: Inactive DBM E7-Heptaglutamate MicroCT Ectopic Bone Formation



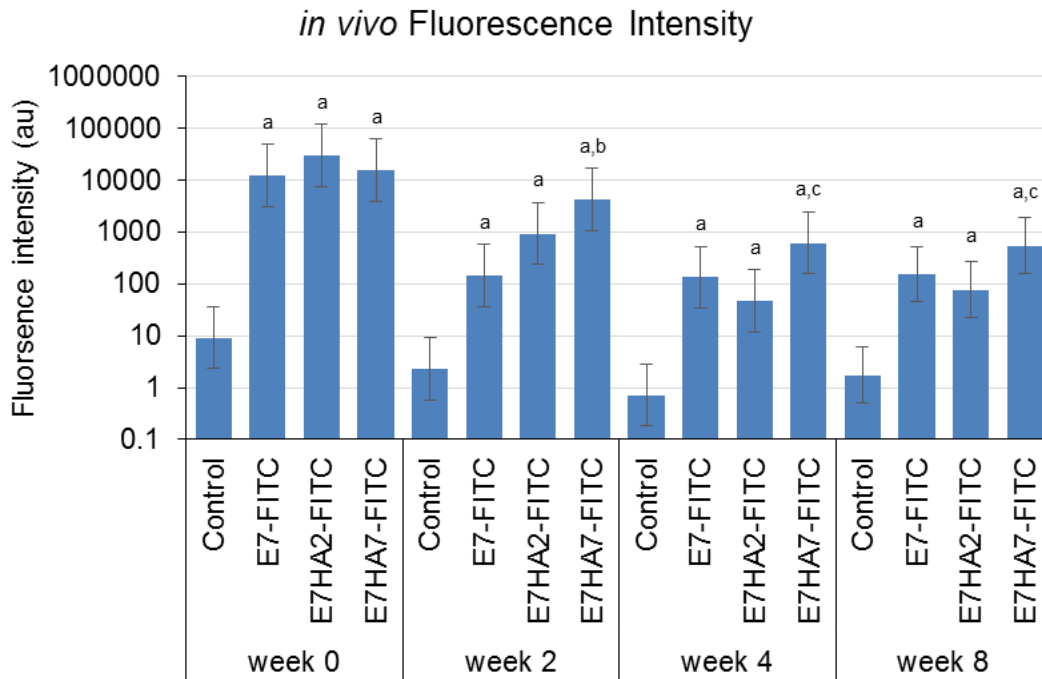
MicroCT rendering of ectopic bone formation. New bone formation can be denoted inside red circle.

Figure 8: Fluorescent Intensity by Peptide Coating Group at Each Week



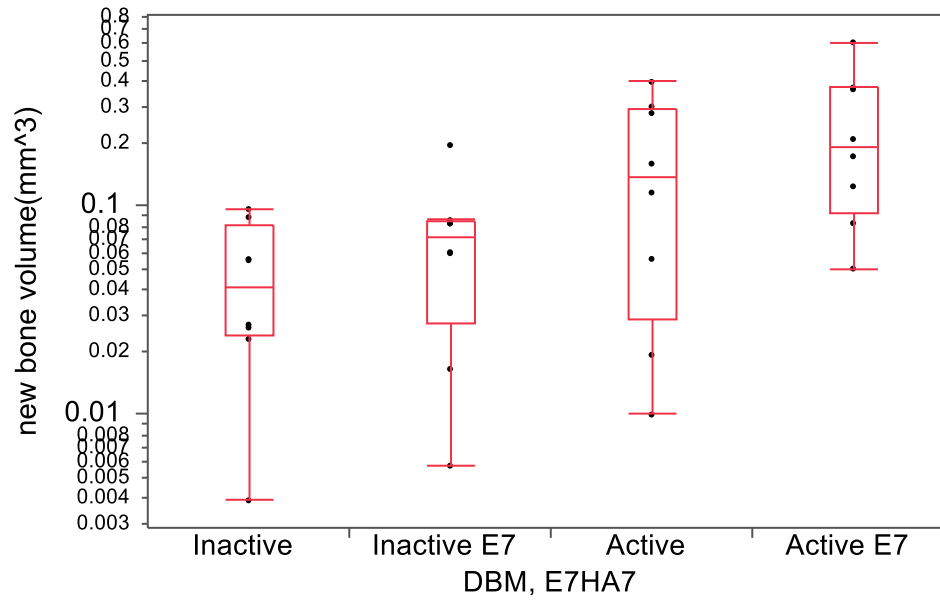
The raw fluorescent intensity of each of the groups at the four-time periods is shown in Figure 8:

Figure 9: Fluorescence Intensity by Peptide Coating Group at Each Week



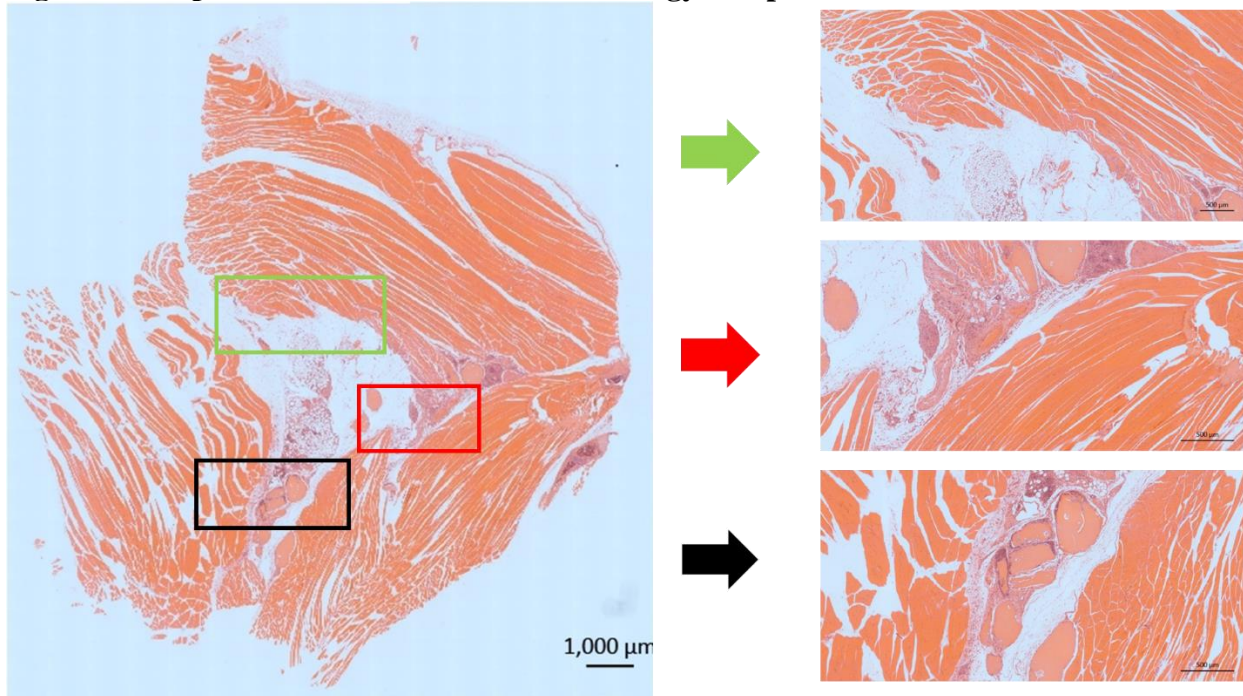
Within each week, differences between the four treatments are identified as follows: The “a” superscript identifies treatments with values significantly different than the control. The “b” superscript identifies differences as compared to E7-FITC. The “c” superscript identifies differences as compared to E7HA2-FITC.

Figure 10: New Bone Volume (mm³) in Ectopic Model



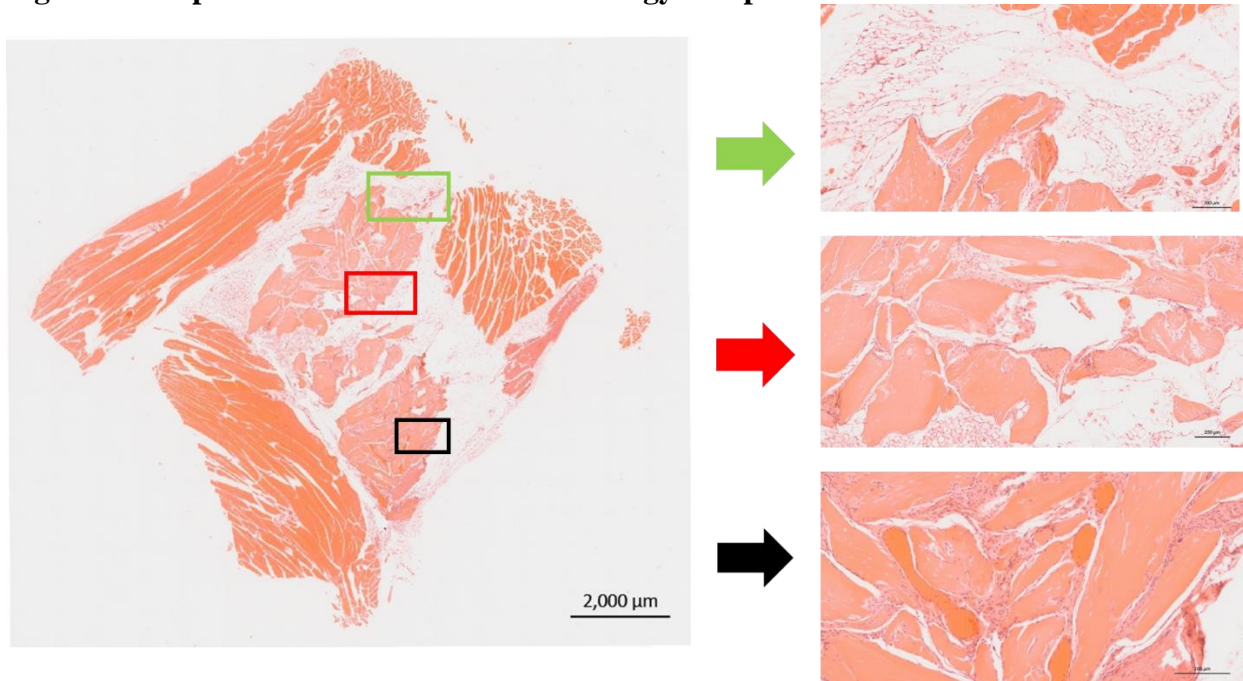
The new bone volume levels in the 16 animals is shown in the boxplots of Figure 10. The median values for the four groups were as follows: Inactive=0.041025 mm³, Inactive E7=0.07135 mm³, Active=0.137985 mm³, and Active E7=0.191515 mm³

Figure 11: Representative Inactive DBM Histology Sample



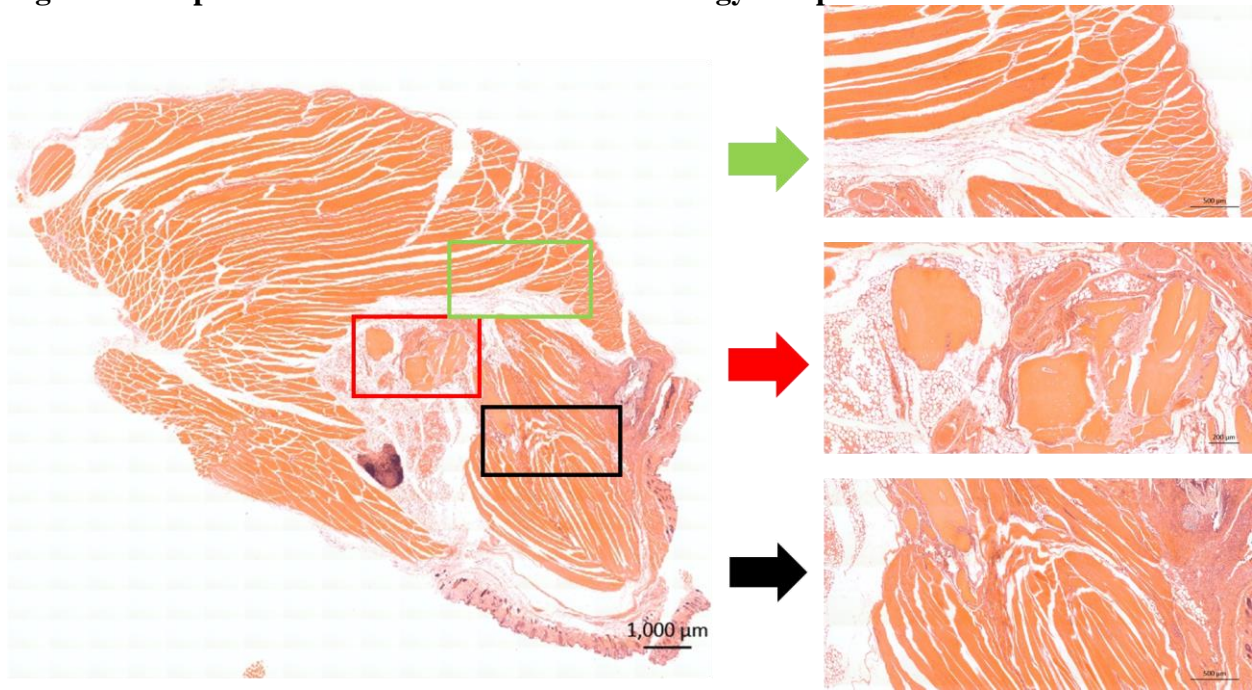
Photomicrographs of iDBM, sample showing DBM particles, surrounded by a combination of connective tissue, adipose tissue, and muscles tissues with lack of new bone formation. (stained with hematoxylin and eosin)

Figure 12: Representative Active DBM Histology Sample



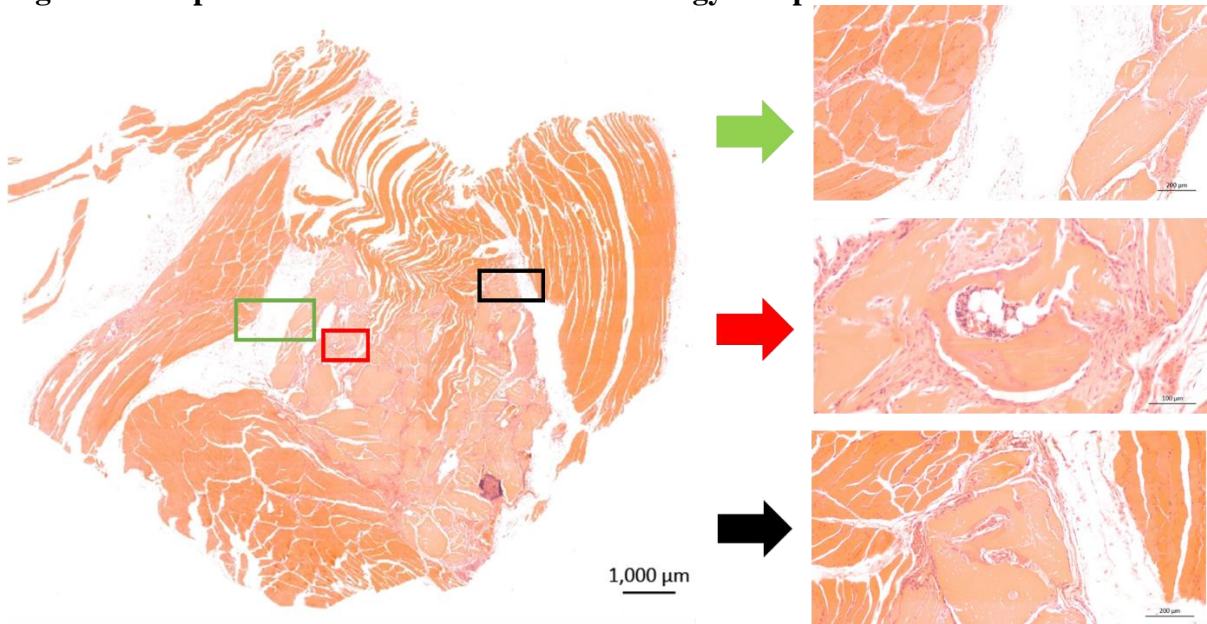
Photomicrographs of aDBM sample showing DBM particles, surrounded by a combination of connective tissue, adipose tissue, and muscles tissues with lack of new bone formation. (stained with hematoxylin and eosin)

Figure 13: Representative Inactive DBM-E7 Histology Sample



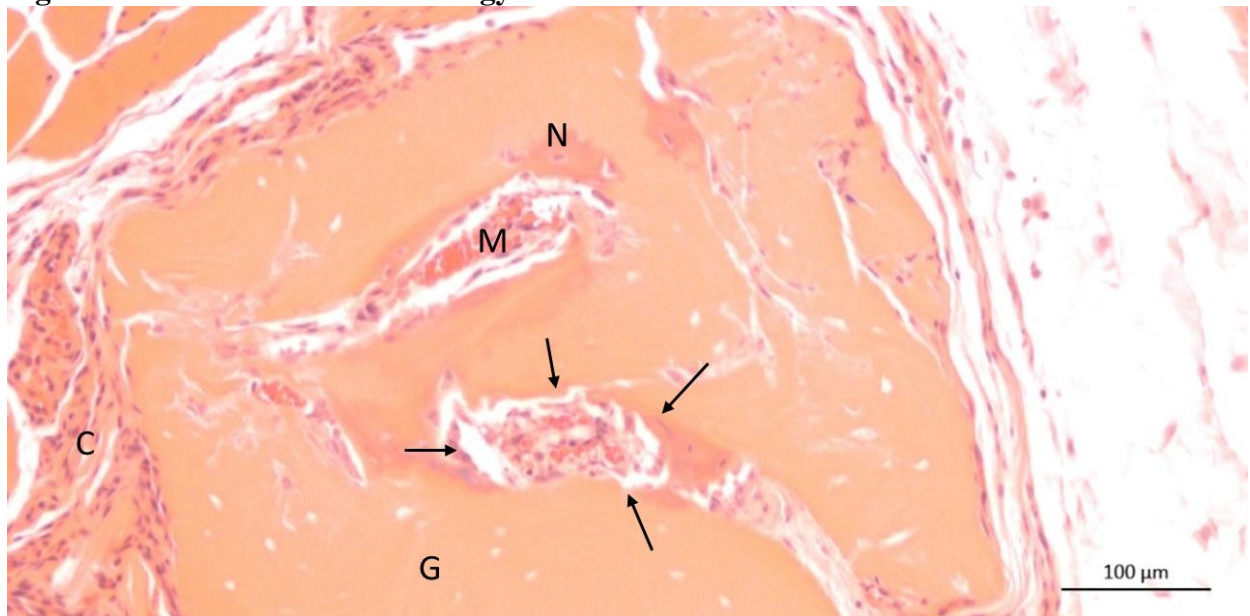
Photomicrographs of iDBM-E7 samples showed DBM particles, surrounded by a combination of connective tissue, adipose tissue, and muscles tissues with lack of new bone formation.

Figure 14: Representative Active DBM-E7 Histology Sample



Photomicrographs of aDBM-E7 showing DBM particles, surrounded by a combination of connective tissue, adipose tissue, and muscles tissues. aDBM-E7 samples showing the presence of ossicles (bone-like tissue surrounding an area of bone marrow-like tissue) in the red and black boxes.

Figure 15: Active DBM-E7 Histology New Bone Formation



Photomicrograph of ossicle formed after intramuscular implantation of DBM 5weeks. Note the Ossicle formed (arrow), New Bone (N), bone marrow (M), Graft (G), Connective Tissue (C). (stained with hematoxylin and eosin)